Electronic supplementary information

A Nickel-foam@carbon-shell with a Pie-like Architecture as an Efficient Polysulfide Trap for High-energy Li-S Batteries

Liu Luo, Sheng-Heng Chung, Chi-Hao Chang and Arumugam Manthiram*
McKetta Department of Chemical Engineering & Texas Materials Institute
The University of Texas at Austin, Austin, TX 78712, USA

Experimental

Preparation of nickel-foam@carbon-shell cathodes: The nickel foam (Pred Materials Inc.) was dispersed in 50 mL hydrochloric acid for 5 min to remove the oxide layer on the surface, followed by washing with water and ethanol and drying in a vacuum oven for 5 h. The pre-treated nickel foam was pressed and cut into a disk with 5 mm in diameter. The mass of the nickel foam is 5.3 mg (areal mass of 27 mg cm^{-2}), and the thickness of the nickel foam is 320 μm. The nickel-foam@carbon-shell cathode was fabricated inside an Ar-filled glove box by incorporating the nickel foam into the carbon shell (7 mm in diameter, Nano Tech Labs), followed by injecting the catholyte into the middle of the nickel foam (5 mm in diameter). The carbon shell utilized in this work weighs 0.73 mg (areal mass of 1.9 mg cm^{-2}). The as-prepared electrode had a sulfur loading of 40 mg cm^{-2} and the weight ratio of sulfur and the other host materials (including nickel foam and carbon shell) is 1.34 : 1 (*i.e.*, ~ 60 wt.% sulfur content). The disadvantage of the use of nickel foam is its relatively higher density than common substrates (like carbon paper), which will lower the energy density of the Li-S cell to some degree. However, the reason why we choose the nickel foam is based on the following advantages. First, the high porosity and conductivity of the nickel

*Corresponding author. Tel: +1-512-471-1791; fax: +1-512-471-7681.
E-mail address: manth@austin.utexas.edu (A. Manthiram)

foam make itself an efficient host to store the active material and promote electron transfer during the charge/discharge process. Second, unlike the commonly used carbon substrates with large micro- and meso-porosity, the metallic nickel foam will not consume a large amount of electrolyte to be sufficiently wetted, which is beneficial to lower the E/S ratio and thus improve the energy density of the Li-S cell. Third, the nickel foam has a good mechanical property, which guarantees the structural integrity of the electrode during long-term cycling.

Assembly of the Li-S cells: Li-S cells (CR2032 coin-type) were assembled inside an Ar-filled glove box with nickel-foam@carbon-shell cathodes and lithium-metal anodes separated by a polypropylene separator (Celgard 2500). 10 μL of the blank electrolyte added on the anode side was 1.85 M $LiCF_3SO_3$ (Acros Organics) and 0.10 M $LiNO_3$ (Acros Organics) in a mixed solvent of dimethoxy ethane (DME, Acros Organics) and 1,3-dioxolane (DOL, Acros Organics) (1:1 v/v). The catholyte used in the cathode was prepared by mixing sublimed sulfur powder (99.5%, Acros Organics) and an appropriate amount of lithium sulfide (Li_2S, 99.9%, Acros Organics) into the blank electrolyte. It was then heated at 50°C in an Ar-filled glove box for 50 h to give 6.0 M sulfur in the form of Li_2S_6 in the solution. The electrolyte/sulfur (E/S) ratio was controlled to be 7 (the electrolyte includes both the polysulfide catholytes and the blank electrolyte added into the anode side) in the Li-S cells. In order to investigate the effect of the nickel-foam@carbon-shell architecture, two types of control cells were assembled with the cathodes: one with the carbon shell only (carbon-shell cathodes) and the other with the nickel-foam only (nickel-foam cathodes).

Assembly of the polysulfide-trap cells: The polysulfide-trap cells were prepared by placing the polypropylene separator – carbon paper – polypropylene separator architecture between the cathode and the lithium-metal anode. The rest of cell-assembly procedures were the same as those of making a regular Li-S coin cell. The inserted carbon paper between the two separators serves as the polysulfide-trap platform to monitor the presence of the polysulfides diffusing from the cathode region and assess the polysulfide-retention level of the specially designed cathodes, *i.e.,* the nickel-foam@carbon-shell electrode architecture.

Electrochemical and microstructural analyses: The Li-S cells with an open-circuit voltage of 2.28 ± 0.02 V were initially charged to 3.0 V followed by discharging and charging in the voltage range of 1.7 – 2.8 V. Cyclic voltammetry (CV) performances were conducted with a universal potentiostat (VoltaLab PGZ 402, Radiometer Analytical) at scan rates of 0.02, 0.05, and 0.1 mV s^{-1} in the potential range of 1.7 – 2.8 V. Surface and bonding characterization were examined with an X-ray photoelectron spectrometer with an Ar^{+}-ion gun for sputtering analysis (XPS, Kratos Analytical Company). XPS spectra decomposition was carried out with a CasaXPS program with Gaussian-Lorentzian functions after the subtraction of the Shirley background. All peaks were calibrated based on the C 1s peak at 284.6 eV. Microstructure analyses were performed with a field-emission scanning electron microscope (FE-SEM, Quanta 650**,** FEI) with an energy-dispersive X-ray spectrometer (EDX) to conduct elemental mapping signals.

Supporting figures

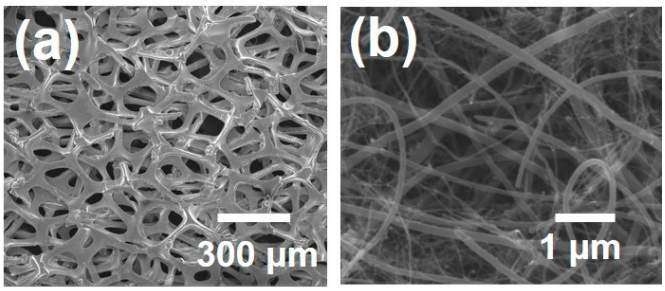

Fig. S1 SEM/EDX inspections of (a) a nickel-foam and (b) a carbon shell from an uncycled nickel-foam@carbon-shell cathode.

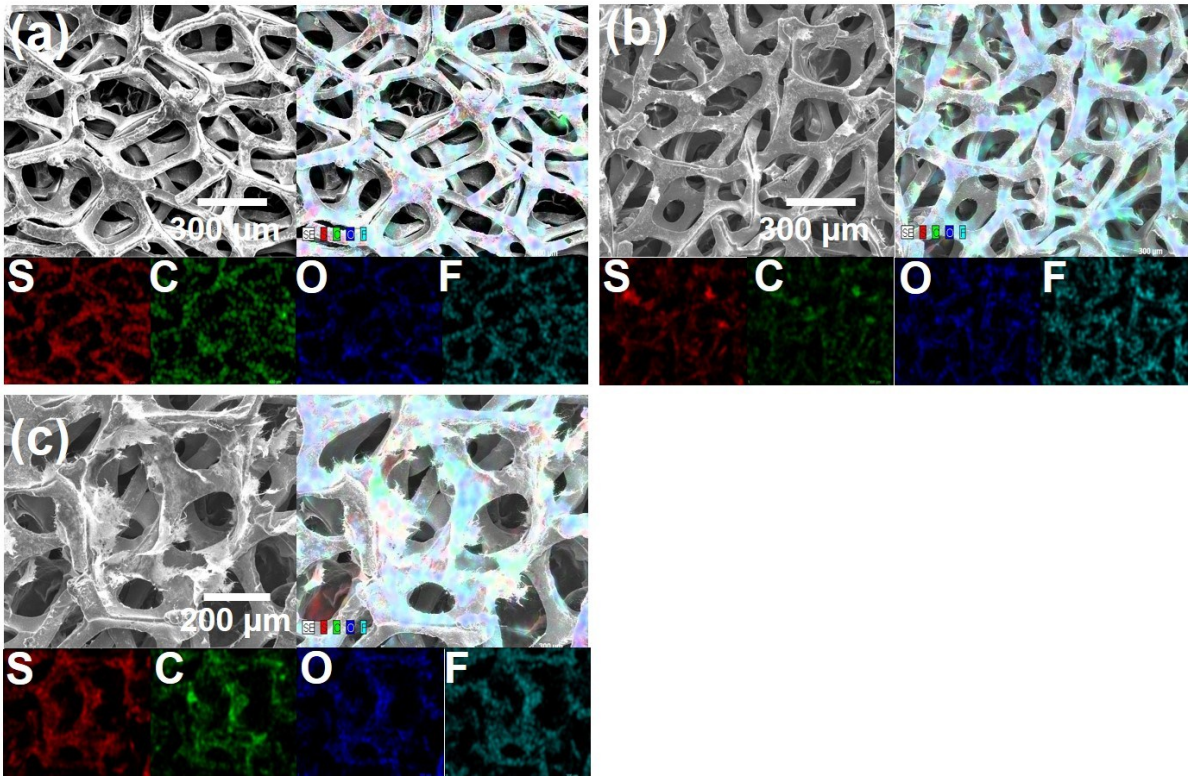

Fig. S2 SEM/EDX inspections of the nickel-foam retrieved from a cycled nickel-foam@carbon-shell cathode under (a) low- and (c) high-magnifications. SEM/EDX inspections of (b) a nickel-foam retrieved from a cycled nickel-foam cathode.

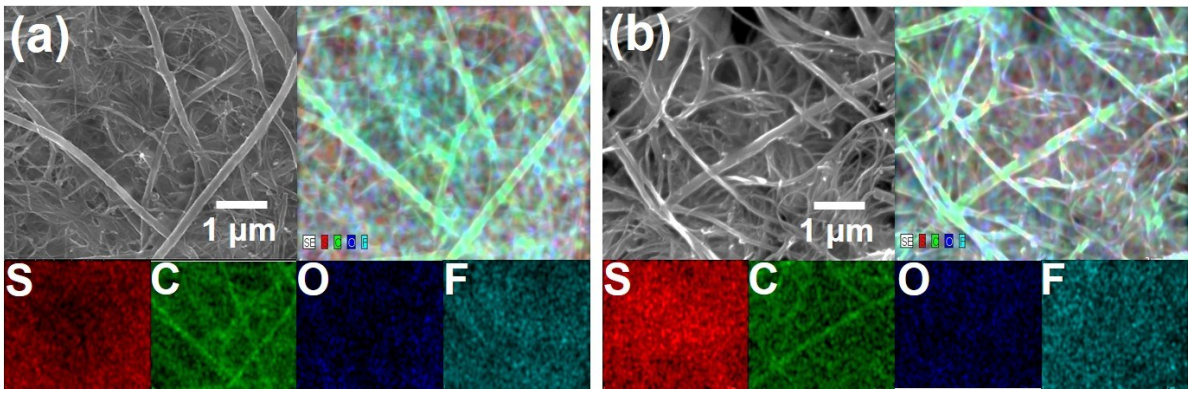

Fig. S3 SEM/EDX inspections of the carbon shell retrieved from (a) a carbon-shell cathode and (b) a nickel-foam@carbon-shell cathode.

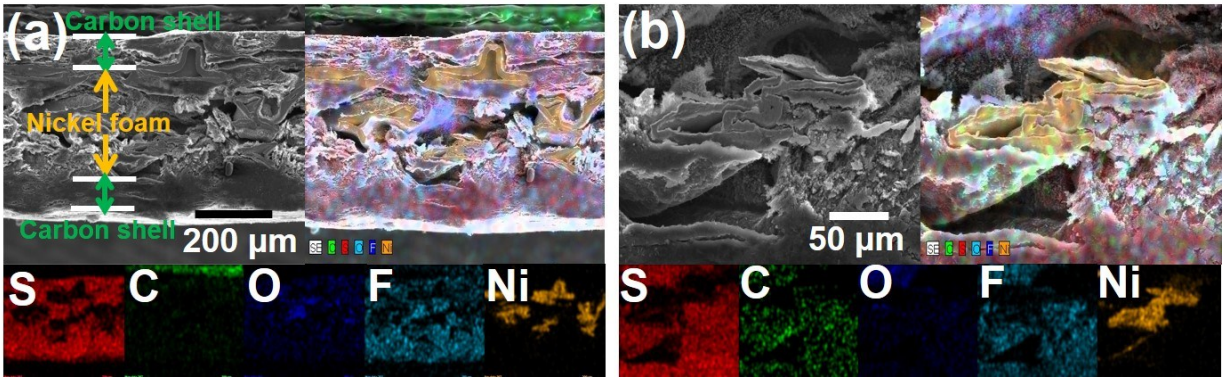

Fig. S4 Cross-sectional SEM/EDX inspections of the cycled nickel-foam@carbon-shell cathode under (a) low and (b) high magnifications.

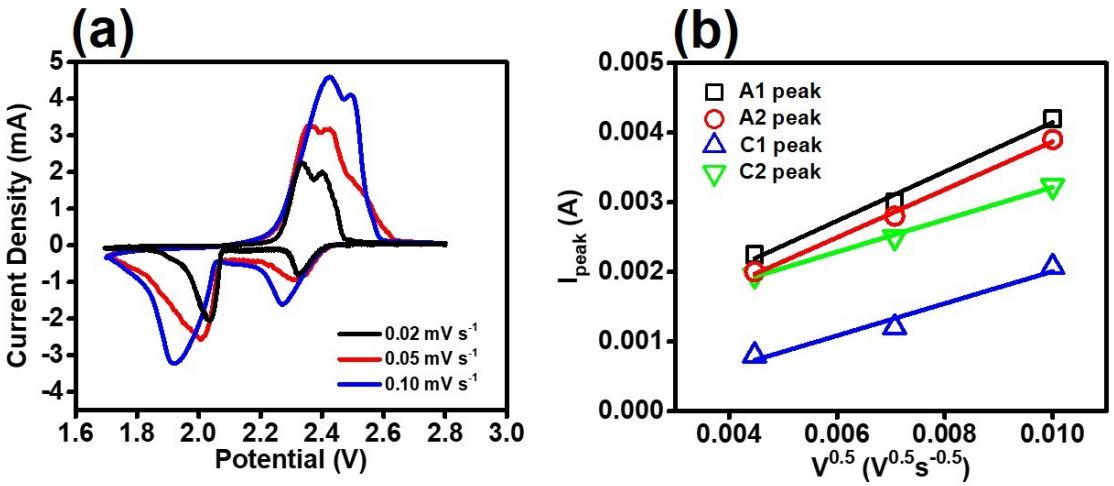

Fig. S5 (a) CV curves of the Li-S cells with the nickel-foam@carbon-shell cathodes at scanning rates of 0.02, 0.05, and 0.1 mV s^{-1}. (b) Linear fitting of the scanning $rate^{0.5}$ based on (a).

Using the linear fitted plots based on the CV curves at different scanning rates, the Li-ion diffusion coefficient (D_{Li^+}) was calculated by the Randles-Sevick equation:[1]

$$I_{peak} = 268600 \times e^{1.5} \times \text{area} \times D_{Li^+}{}^{0.5} \times \text{concn}_{Li^+} \times \text{rate}^{0.5}$$

where I_{peak} is the current of the peak, e is the number of electrons, area refers to the cathode area, concn._{Li^+} refers to the Li-ion concentration in the electrolyte, and rate refers to the CV scanning rate. As a result, the D_{Li^+} values at two anodic peaks (A1 and A2) and cathodic peaks (C1 and C2) are, respectively, 2.26×10^{-8}, 2.20×10^{-8}, 9.68×10^{-9}, and 9.73×10^{-9} cm^2 s^{-1}.

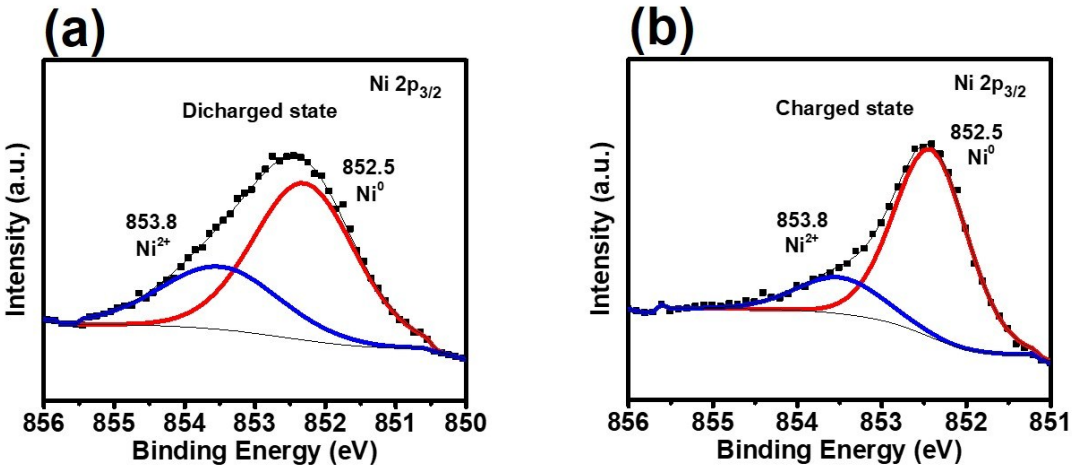

Fig. S6 Ni $2p_{3/2}$ XPS spectra of the nickel-foam in the nickel-foam@carbon-shell cathode at (a) discharged state and (b) charged state.

From the deconvoluted $2p_{3/2}$ peak of Ni, the presence of Ni^{2+} at 853.8 eV in the form of NiS[2,3] indicate the interaction between Ni and polysulfides during the discharge process. During charge, the content of Ni^{2+} is lower than that during discharge, further confirming the contribution from Ni to adsorb polysulfide species and confine them on the electrode surface during discharge and to help reversible conversion to transform polysulfides to elemental sulfur during the charge process.

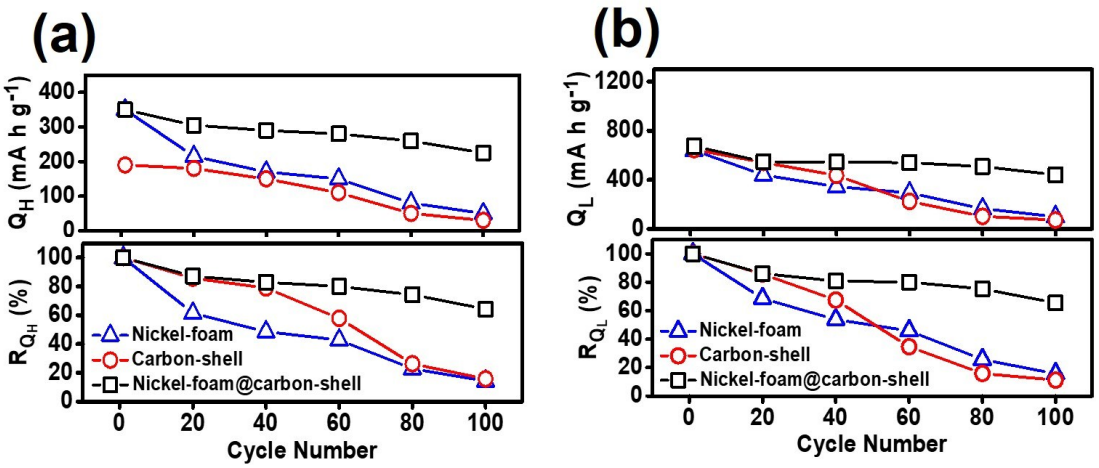

Fig. S7 (a) Q_H and R_{QH} analysis. (b) Q_L and R_{QL} analysis.

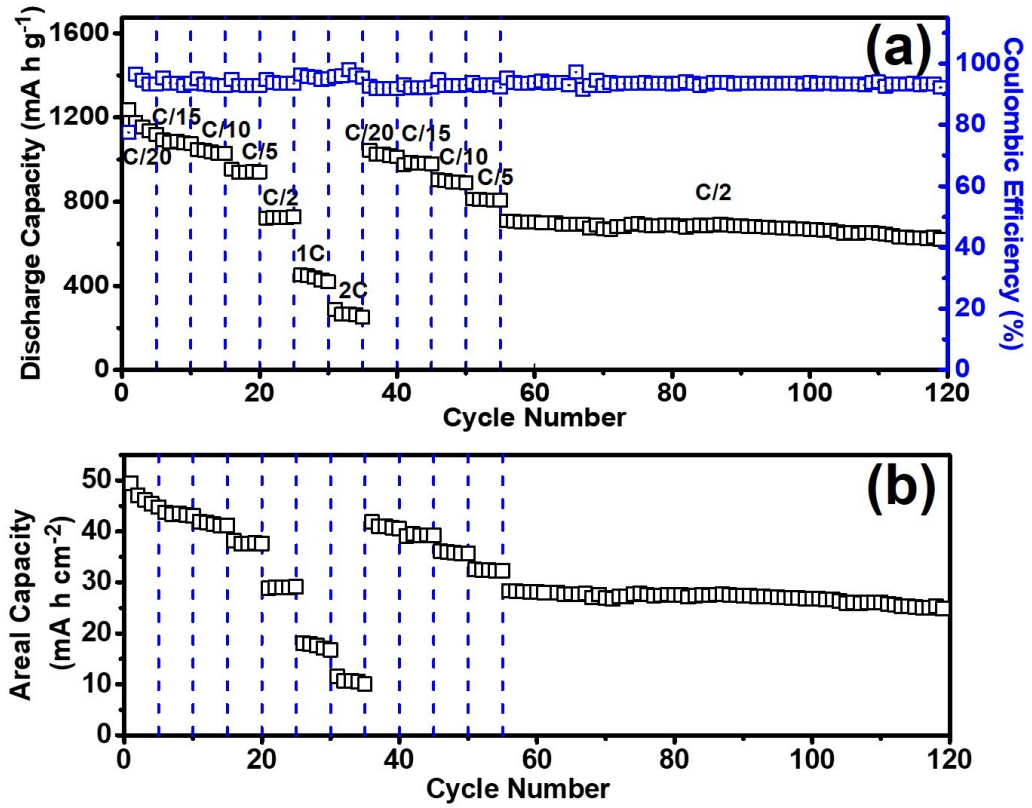

Fig. S8 (a) Cycling performance and (b) corresponding areal capacity of the cell with the nickel-foam@carbon-shell cathode at different cycling rates.

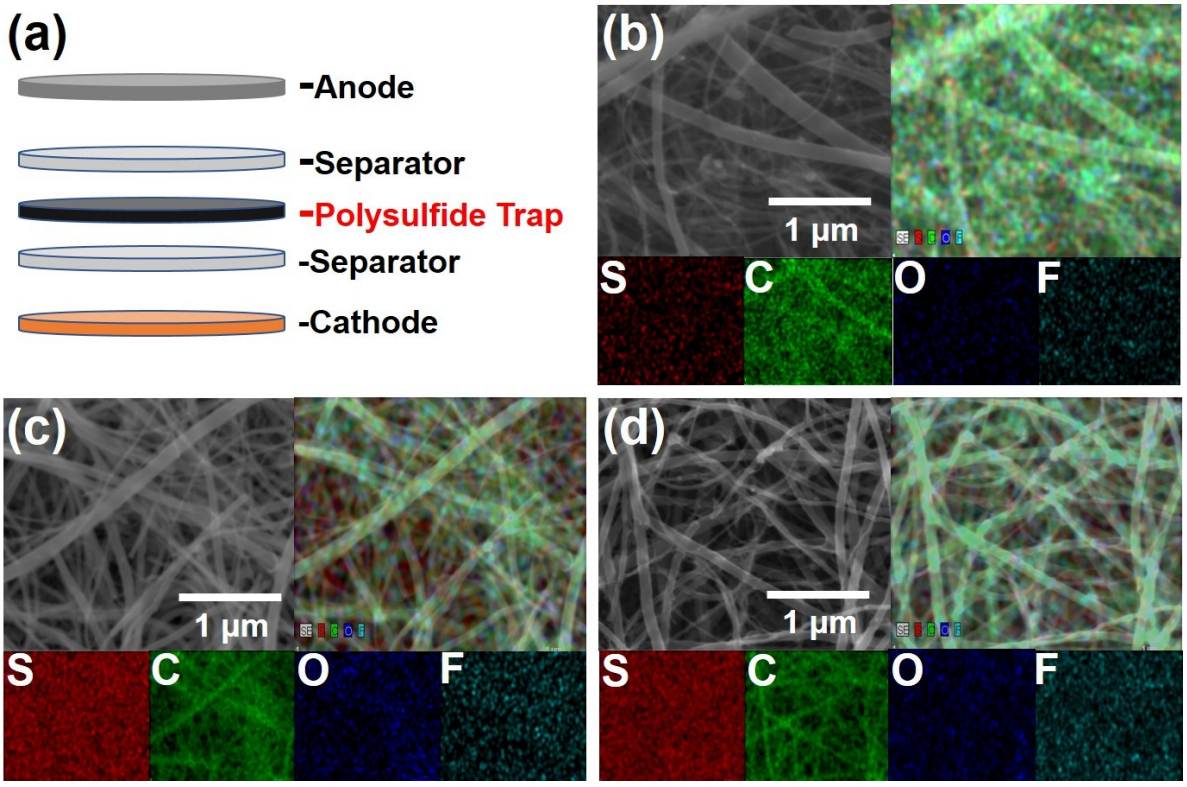

Fig. S9 (a) Illustration of the configuration of the polysulfide-trap cell. SEM/EDX inspections of the cycled polysulfide traps from (b) nickel-foam@carbon-shell cathode, (c) carbon-shell cathode, and (d) nickel-foam cathode.

Table S1 Relative areas of different sulfur peaks in the S 2p XPS of the carbon-shell and nickel-foam@carbon-shell cathodes.

Carbon-shell cathode		Nickel-foam@carbon-shell cathode	
Position (eV)	% Area	Position (eV)	% Area
160.0	53.40	160.4	34.04
161.2	26.70	161.6	17.01
161.5	10.02	161.8	22.70
162.7	5.18	163.0	11.35
163.0	3.13	163.4	6.61
164.2	1.57	164.6	8.29

Table S2 Relative areas of the different nickel peaks in the Ni $2p_{3/2}$ XPS of the nickel-foam@carbon-shell cathode at discharge and charged states.

Discharged state		Charged state	
Position (eV)	% Area	Position (eV)	% Area
852.5	67.99	852.5	81.48
853.8	32.01	853.8	18.52

References

1 J.-Q. Huang, Q. Zhang, H.-J. Peng, X.-Y. Liu, W.-Z. Qian, F. Wei, *Energy Environ. Sci.*, 2014, **7**, 347-353.

2 L.-J. Liu, Y. Chen, Z.-F. Zhang, X.-L. You, M. D. Walle, Y.-J. Li, Y.-N. Liu, *J. Power Sources*, 2016, **325**, 301-305.

3 D. L. Legrand, H. W. Nesbitt, G. M. Bancroft, *Am. Mineralogist*, 1998, **83**, 1256-1265.